A&A 409, 899–906 (2003)
DOI: 10.1051/0004-6361:20031219

Astronomy & Astrophysics

Low signal-to-noise spectroscopy and surface photometry of two faint galaxies in the field of NGC 7479

M. F. Saraiva[1] and G. F. Benedict[2]

[1] Departamento de Astronomia, Instituto de Física, Universidade Federal do Rio Grande do Sul, Av. Bento Gonçalves 9500, CP 15051, 91501-970 Porto Alegre, RS, Brasil
[2] Department of Astronomy and McDonald Observatory, University of Texas at Austin, Austin, Texas 78712-1083, USA
e-mail: fritz@astro.as.utexas.edu

Received 16 April 2003 / Accepted 29 July 2003

Abstract. We present low signal-to-noise spectroscopy and surface photometry of two small galaxies, detected in the field of the nearby asymmetric barred spiral NGC 7479, near a prolongation of the western arm that forms a faint tail in the disc, and selected as possible companions of this galaxy. The analysis was based on data obtained with the Prime Focus Camera (PFC) at the 0.8 m telescope of McDonald Observatory, and the Low Resolution Spectroscope (LRS) at the 9.2 m Hobby-Eberly Telescope (HET). We determined radial velocities using cross correlation with 15 different templates, and derived integrated magnitudes, colors and brightness profiles for each.
The derived radial velocities are around 35 500 km s^{-1} for one galaxy and 38 000 km s^{-1} for the other, which clearly indicates that both are far more distant than the nearby NGC 7479. The absolute magnitudes and diameters of these two background galaxies are typical of normal galaxies, and their colors are similar to other galaxies with similar redshifs. NGC 7479 continues to exist in isolation with no detected companion.

Key words. galaxies: individual: NGC 7479 – galaxies: photometry

1. Introduction

NGC 7479 is a grand-design spiral galaxy, classified as SB(s)c in RC3 (de Vaucouleurs et al. 1991), that has been extensively studied for its impressive features. It has an unusually strong bar, with dust lanes associated with molecular gas, detected in CO, and regions of intense star formation (e.g. Benedict 1982; Quillen et al. 1995; Sempere et al. 1994; Martin & Friedli 1997; Rozas et al. 1999; Aguerri et al. 2000. These last authors cataloged more than 1000 HII regions in the galaxy, including bar and disc. The spiral structure has as main components two spiral arms strongly asymmetric (Martin & Friedli 1997), that apparently are leading (Beckman & Cepa 1990; Puerari & Dottori 1997), and present strong 21-cm line emission (Laine & Gottesman 1998). The small and bright nucleus is classified as LINER by Keel (1983) and as Seyfert 1.9 by Ho et al. (1997). It presents a circumnuclear disc detected in CO (Sempere et al. 1994; Laine et al. 1999) and in HI (Laine & Gottesman 1998). The infrared colors of the galaxy are typical of galaxies having bursts of star formation.

The overall morphology of the galaxy seems to be an excellent example of an interacting system, but it has no close companion, leading some authors (e.g. Quillen et al. 1995; Laine & Gottesman 1998; Martin et al. 2000) to propose a model in which NGC 7479 would have suffered a recent merger with a low mass galaxy. This merger became even more likely after the simulations by Laine & Heller (1999) in which they reproduce the appearance of the galaxy supposing it captured a small companion in a canibalization process that may not be completed yet.

In an attempt to find low surface brightness galaxies in the neighborhood of NGC 7479, we had several runs in 1995 with the Prime Focus Camera at the 0.8 m telescope of McDonald Observatory to obtain long exposure, wide field images of the galaxy. We found no companion. In a recent re-examination of the those images, we identified some features that might had added new evidence for the merger hypothesis. These images, after a very precise sky subtraction, reveal a prolongation of the western arm beyond the disc edge that forms a faint tail, not shown in any previous image of NGC 7479. Close to the tail, there are two very small faint galaxies. These features are shown in Fig. 1.

If these galaxies were at the same distance as NGC 7479, they could be tidal dwarf galaxies, a type of object that may be produced during galactic encounters (Duc & Mirabel 1998).

This possibility prompted us to ask for time at the HET telescope to obtain spectra of the galaxies to measure their radial velocities. This would allow us to determine if they are dwarf

Send offprint requests to: M. F. Saraiva,
e-mail: fatima@if.ufrgs.br

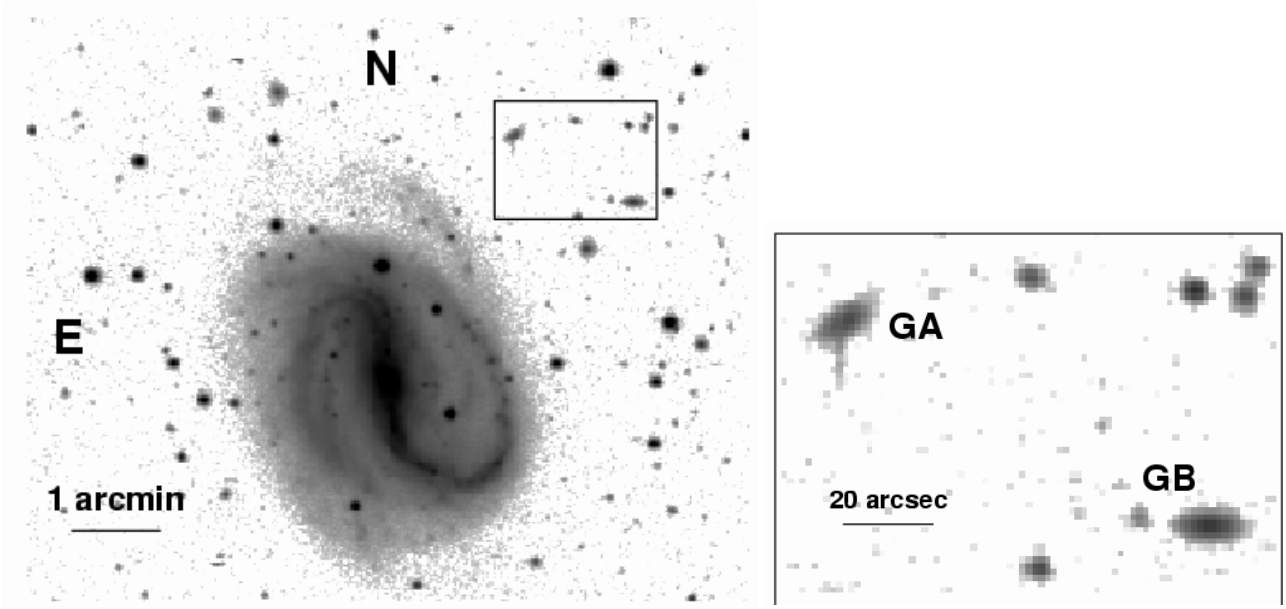

Fig. 1. The left panel shows NGC 7479 and, in the marked region, the two faint galaxies, that we will call NGC 7479-GA and NGC 7479-GB, or GA and GB for short. This region appears zoomed in the right panel, showing GA at top left and GB at bottom right. The J2000 equatorial coordinates of the galaxies are $\alpha = 23:04:50.8$, $\delta = 12:22:08.4$, and $\alpha = 23:04:45.3$, $\delta = 12:21:24.6$, for GA and GB respectively. The 2MASS Extended Source Images (NASA/IPACInfrared Science Arquive (IRSA), has recently released observational results on GB: its identification is 2MASXJ23044541+1221233, and its total magnitudes are $J = 15.259 \pm 0.230$, $H = 14.384 \pm 0.198$, and $K_s = 13.744 \pm 0.258$(NED).

companions of NGC 7479 or normal, more distant galaxies. In this paper we present those observations, in Sect. 2, the results from spectroscopy, in Sect. 3, and from surface photometry, in Sect. 4. In Sect. 5 we summarize our results.

2. Observations and data reductions

2.1. Photometric data

The photometric data were obtained at McDonald Observatory, using the 0.8-m telescope with the Prime Focus Camera (PFC). The detector was a 2048×2048 CCD with pixel size of 15 μ, corresponding to a plate scale of 1.35 arcsec pix^{-1}. The field of view was $46 \times 46\,\square'$. The filters used were B, V, R and I. Multiple exposures of standard stars from Landolt (1992) were also taken for the photometric calibration.

The images were corrected for bias and flat-field using standard IRAF routines. After the correction by atmosferic extinction the multiple exposures in each filter have been aligned and combined. The alignments were correct within 0.25 pixel in average. The sky background of each final broad-band image has been determined with the IRAF routine *imsurfit*, by fitting a 2nd order polynomial to the frame regions around the galaxy, after cleaning all the stars on them. The calculated sky values and their uncertainties are shown in Table 1.

The data was calibrated to the Johnson-Kron-Cousins system using observations of standard stars in the regions SA92 and SA97 of Landolt (1992). The transformation equations are given in another paper (Saraiva & Benedict 2003, in preparation).

Table 1. Photometric observations.

Filter	*FWHM* arcsec	Exposure time s	Sky brightness μ
B	3.0	3×600	22.34 ± 0.027
V	2.7	2×600	21.39 ± 0.021
R	2.7	3×300	20.75 ± 0.011
I	3.1	3×600	19.37 ± 0.012

Table 2. Spectroscopic observations

Slit width arcsec	Exposure min	Spectral range Å	Resolution Å
2	2×10	4300–7300	4

2.2. Spectroscopic data

The spectroscopic data were obtained with the Low Resolution Spectrograph (LRS) at the 9.2 m Hobby-Eberly Telescope (HET). The detector is a 1568×512 CCD binned 2×2, corresponding to a plate scale of 0.47 arcsec pix^{-1}. We used a grating of 600 l/mm, a slit width of 2 arcsec, and the filter GG385. The obtained resolution with this setup is 4 Å, and the spectral coverage is 4300–7300 Å . The slit has total length of 4 arcmin and was properly oriented to include both galaxies. Two exposures of 10 min each were taken.

The data reduction, consisting of bias subtraction, flat-fielding, sky subtraction, and wavelength calibration was

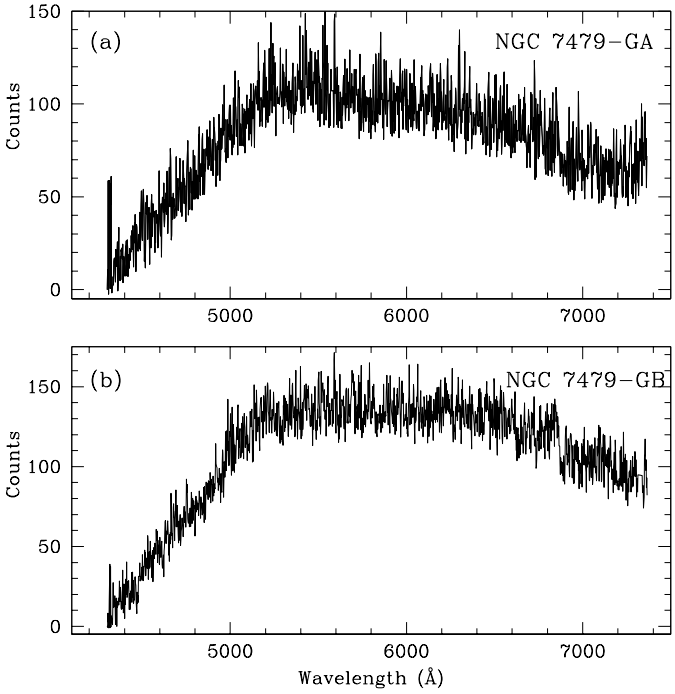

Fig. 2. a) Spectrum of NGC 7479-GA. The ordinate is the number of counts per pixel. **b)** Spectrum of NGC 7479-GB.

carried out using standard IRAF[1] routines. The cosmic rays were eliminated using the IRAF task *cosmic ray* prior to the spectra extraction, and the remaining ones have been eliminated by interpolation. The extraction window for each galaxy has been chosen to include the total galaxy appearing in the slit. The combination of the spectra was made after the extractions. The signal-to-noise after the combination was 8.5 for the galaxy A and 13.5 for the galaxy B, in the range 6000–6500 Å. Figure 2 shows the spectra.

3. Spectroscopy

3.1. Cross-correlation

For determining the radial velocities we used the IRAF task *fxcor*, that applies the Fourier Cross Correlation technique, as described in Tonry & Davis (1979 – hereafter TD79). Basically, the galaxy spectrum is correlated against the template spectrum and the resultant peak is fit by a smooth symmetric function.

Although usually stellar spectra are used as templates, in the case of poor signal-to-noise data, which is our case, galaxy spectra are more appropriate (TD79). We used three sets of galaxy templates: the first one is composed by the spectra of three elliptical galaxies (NGC 6851, NGC 6958 and ESO 185-54) and one SO galaxy (IC 4214), taken at the Laboratório Nacional de Astrofísica, Brazil (LNA). Initially we tried to include in this set the spectra of two spiral galaxies (NGC 5757 and NGC 7412) but the correlation with these galaxies was very poor, so we dropped them. The four template spectra used have good signal-to-noise, are normalized and shifted to zero redshift. Details on their characteristics are given in Saraiva et al. (2001).

The second set is composed by Las Campanas spectra of the elliptical galaxies NGC 1700, NGC 1426, and NGC 1407, plus a synthetic galaxy spectrum. These spectra have high signal-to-noise and are not shifted to zero redshift, with the obvious exception of the synthetic one.

The third set is composed by galaxy templates built from star clusters integrated spectra (Bica 1988).

Due to the very poor signal-to-noise of our object spectra, the true peak of the correlation was not easily recognized. In some cases there were other peaks of similar height. As recommended by TD79 we chose as main peak the one that showed up best (highest amplitude) in all the correlations.

3.2. Radial velocities

Tables 3, 4 and 5 summarize the correlation results for GA and GB. The parameters listed are the height of the chosen peak (Height), the ratio of the chosen peak to the average peak of the cross correlation function (R), the *FWHM* of the peak (Width), the velocity computed from the shift (Relative velocity), and the resulting velocity (Observed velocity). The two last columns have the same values if the template spectra have zero redshift, which is the case of first and third set.

Figures 3 and 4 show the cross-correlation of NGC 7479-GA and NGC 7479-GB with NGC 6851. The cross-correlation functions of the two galaxies with the other templates have nearly the same shape and values.

Although in most cases the R value is very small, and the computed velocity has a large internal uncertainty, all the 15 correlations computed for each galaxy gave practically the same result, which make us confident it is correct. The mean resulting radial velocities are $(35\,926 \pm 413)$ km s^{-1} for NGC 7479-GA and $(38\,009 \pm 83)$ km s^{-1} for NGC 7479-GB.

4. Surface photometry

In spite of the very low signal-to-noise ratio of the galaxies, we were able to calculate some photometric parameters, specifically diameters, ellipticities, position angles, integrated magnitudes and colors, and surface brightness profiles along the major axis.

4.1. Ellipse fits

In order to be able to determine geometric parameters using the task *ellipse* in the STSDAS package for IRAF, we artificially increased the resolution of each galaxy image, to have a number of points large enough to allow the calculation of the ellipses. We have done that using the IRAF task *magnify*, with a magnification factor of 10. We used these magnified images only for the purpose of obtaining the isophote parameters, all the remaining analyses were based on the original images.

Figure 5 shows the variation of the surface brightness (μ), ellipticity (ϵ), position angle of the major-axis (PA), and the

[1] IRAF – Image Reduction and Analysis Facility – is distributed by the National Optical Astronomy Observatories, which is operated by the Association of Research in Astronomy, Inc., under cooperative agreement with the National Science Foundation, USA.

Table 3. Correlation results for the first set.

Galaxy	Template	Height	R	Width km s^{-1}	Relative velocity km s^{-1}	Observed velocity km s^{-1}
N 7479-GA	N 6851	0.123	3.428	3011	35 957	35 957 ± 534
N 7479-GA	N 6958	0.112	2.808	2922	35 842	35 842 ± 602
N 7479-GA	I 4214	0.104	2.945	1371	36 034	36 034 ± 664
N 7479-GA	E 185-G54	0.114	2.847	4788	36 112	36 112 ± 977
N 7479-GB	N 6851	0.235	2.721	2977	37 920	37 920 ± 628
N 7479-GB	N 6958	0.227	2.939	2540	38 100	38 100 ± 506
N 7479-GB	I 4214	0.210	2.925	2319	38 040	38 040 ± 464
N 7479-GB	E 185-G54	0.196	2.33	2712	38 232	38 232 ± 638

Table 4. Correlation results for the second set.

Galaxy	Template	Height	R	Width km s^{-1}	Relative velocity km s^{-1}	Observed velocity km s^{-1}
N 7479-GA	N 1407	0.220	3.46	1902	34 456	35 896 ± 334
N 7479-GA	N 1426	0.139	3.11	844	33 151	34 798 ± 161
N 7479-GA	N 1700	0.152	2.95	1051	30 526	34 888 ± 300
N 7479-GA	*synth*	0.157	3.77	1254	34 987	34 987 ± 206
N 7479-GB	N 1407	0.404	10.58	3020	36 020	37 986 ± 331
N 7479-GB	N 1426	0.282	2.184	1289	36 370	38 031 ± 169
N 7479-GB	N 1700	0.362	5.256	1973	33 544	37 925 ± 212
N 7479-GB	*synth*	0.28	5.18	1037	37 965	37 965 ± 98

Table 5. Correlation results for the third set.

Galaxy	Template	Height	R	Width km s^{-1}	Relative velocity km s^{-1}	Observed velocity km s^{-1}
N 7479-GA	E1	0.148	3.217	2840	35 549	35 549 ± 529
N 7479-GA	E2	0.154	3.132	3030	35 425	35 425 ± 576
N 7479-GA	E3	0.156	3.159	3561	35 623	35 623 ± 672
N 7479-GA	E4	0.162	4.053	1757	35 187	35 187 ± 273
N 7479-GA	E5	0.168	3.665	3592	35 487	35 487 ± 604
N 7479-GA	E6	0.184	3.751	3705	36 484	36 484 ± 612
N 7479-GA	E7	0.168	3.756	2938	35 429	35 429 ± 485
N 7479-GB	E1	0.216	3.238	2086	37 982	37 982 ± 386
N 7479-GB	E2	0.263	3.103	2130	37 961	37 961 ± 407
N 7479-GB	E3	0.278	4.856	2078	38 071	38 071 ± 278
N 7479-GB	E4	0.184	2.917	1279	37 927	37 927 ± 257
N 7479-GB	E5	0.244	2.995	2115	37 940	37 940 ± 415
N 7479-GB	E6	0.340	4.956	2224	38 025	38 025 ± 293
N 7479-GB	E7	0.277	3.515	1907	38 044	38 044 ± 331

$\cos 4\theta$ term, with the 1/4 power of the ellipse semi-major axis ($a^{1/4}$).

These diagrams are significant only for $a^{1/4} \geq 1.1$ ($a \geq 1.5$) since the real resolution is 1.35″. We can see that, in the significant range, GB presents smooth and coherent variations in the four filters, while in GA the isophotes are clearly more disturbed, with parameters varying differently in the different filters. Particularly, the position angle of the inner isophotes in the V filter (triangles) presents a shift of 10° with respect to the other filters.

We adopted as PA and ϵ of the galaxies the values obtained from the average of the fittings to the outermost isophotes in the four filters. The values for GA are PA = 119° and $\epsilon = 0.44$, and for GB are PA = 87° and $\epsilon = 0.52$. The shape parameter, $B4$, indicates that GB has disky isophotes, but does not allow us to take any conclusion for GA.

4.2. Luminosity profiles

The surface brightness, shown in Fig. 6, span a range of three magnitudes. The observed central surface brightness is $\mu_B \simeq 23.3$ for both galaxies. Their major axes at $\mu_B = 26$, measured in these profiles, are 14″ (GA) and 18″ (GB). The shape of the color profiles are almost totally masked by the errorbars, but

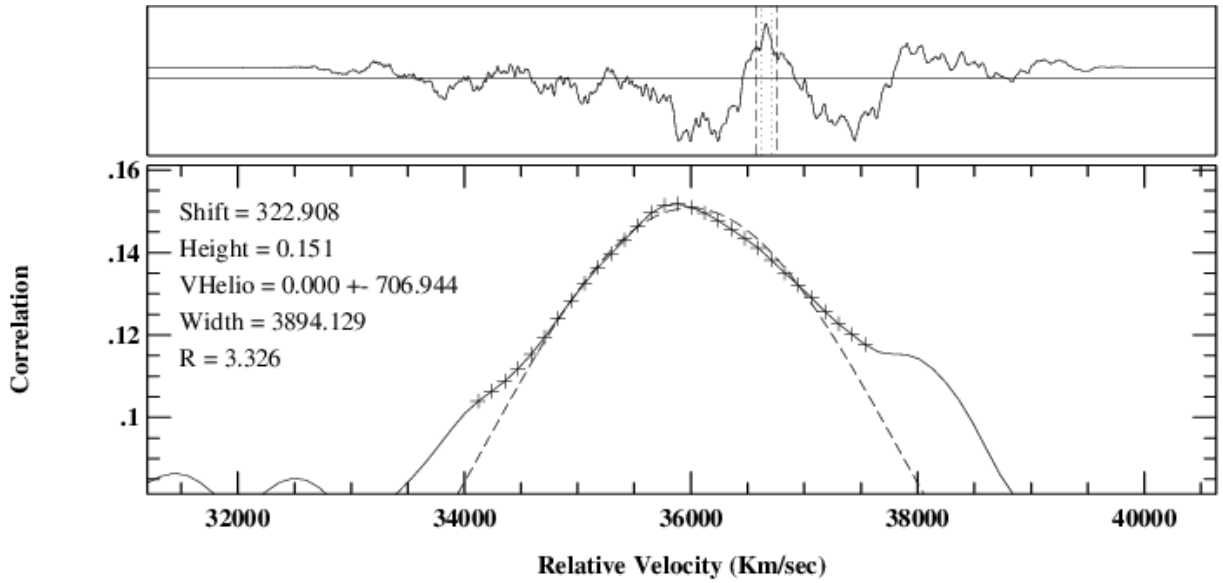

Fig. 3. The top panel is the cross-correlation function of NGC 7479-GA with NGC 6851, with the main peak between dashed lines. The bottom panel shows the fitting of the main peak.

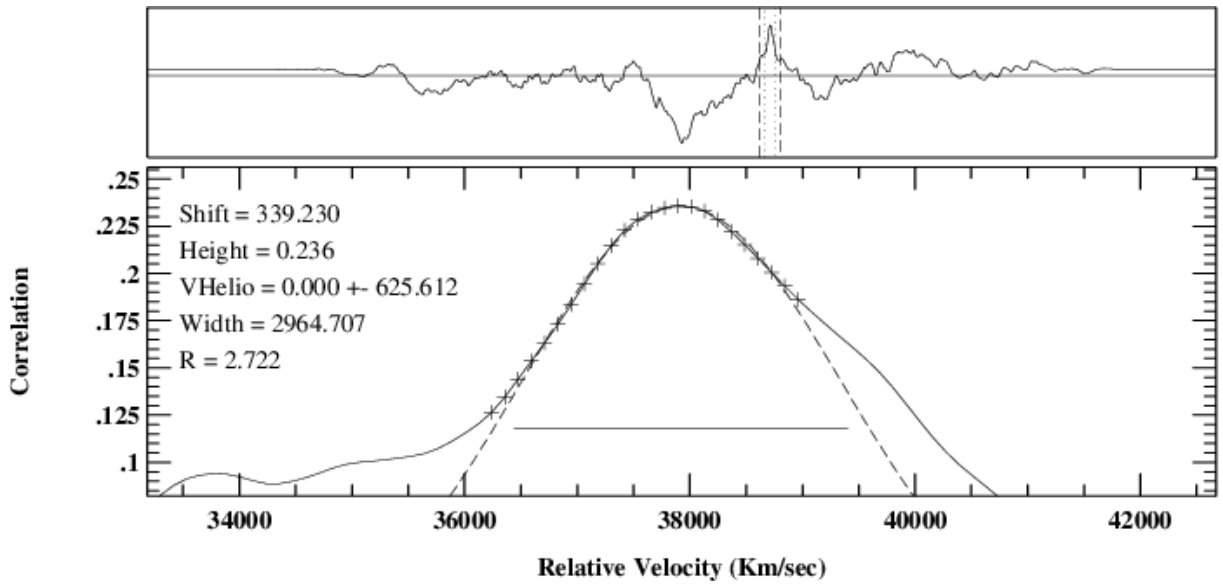

Fig. 4. Cross correlation of NGC 7479-GB with NGC 6851.

they still allow to notice that GB has a smooth surface brightness distribution, while GA seems to have some inner feature that disturbs its brightness distribution and causes the asymmetry in their color profiles. This might be an indication that the morphological type of GA is later than GB.

4.3. Integrated magnitudes

The integrated magnitudes were calculated within apertures of 10.8 and 13.5 arcsec for both galaxies, and the corresponding colors were obtained.

These apertures were selected attempting to include the maximum flux with the minimum noise, for which we used the criterium that the aperture should be the closest one to twice the *FWHM* of the corresponding galaxy.

These parameters were corrected for Galactic extinction, adopting the values for NGC 7479 from Schlegel et al. (1998), from NED, and for redshift (k-correction), interpolating from tables provided by Poggianti (1997) for types E, Sa and Sc (Brown et al. 2001).

The adopted Galactic extinction values are $A_B = 0.482$, $A_V = 0.370$, $A_R = 0.299$, and $A_I = 0.217$, and the interpolated k-correction values for $z = 0.12$ are $k_B = 0.52$, $k_V = 0.173$, $k_R = 0.10$, and $k_I = 0.037$. These k_B and k_V values are intermediate between those given in Whitford (1971) and to those obtained following RC3 (de Vaucouleurs et al. 1991) for morphological type Sa ($T = 1$).

The integrated magnitudes and colors of the two galaxies are shown in Table 6. The quoted errors refer to the internal uncertainty in the measurement of the magnitude, due to uncertainties in the sky subtraction, and in the case of colors were

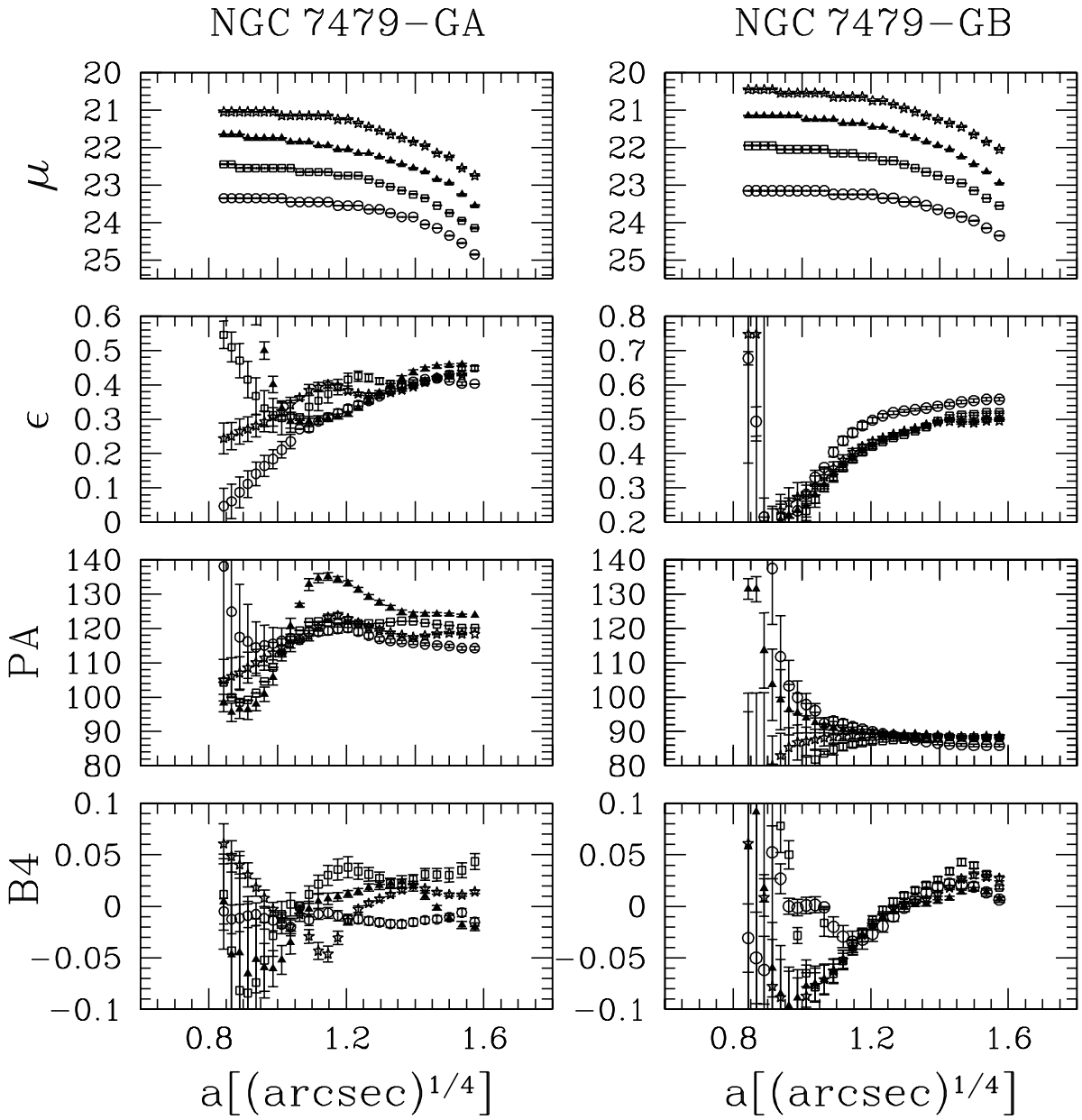

Fig. 5. Isophotal parameters surface brightness (μ), ellipticity (ϵ), position angle (PA), and $\cos 4\theta$ Fourier term ($B4$), as a function of the semi-major axis ($a^{1/4}$). The symbols circles, squares, triangles, and stars, represent the filters B, V, R, and I, respectively.

calculated as the sum in quadrature of the uncertainty in each magnitude. The integrated parameters show that GB is slightly brighter and significantly redder than GA, mainly in $B-V$, what is in agreement with the local color profiles.

Comparing the corrected colors with the mean *BVRI* colors of nearby galaxies, (e.g. Buta & Willians 1995; Marakova 1999) both GA and GB have nontypical colors, mainly GA, that is both blue in $B-V$ and red in $V-I$. Probably a best comparison sample is provided by Bershady et al. (1994), who present *UJFNK* colors of galaxies at $z \leq 0.25$, with median $z = 0.12$. Since these authors made no correction for reddening or redshift, we used our uncorrected *BVRI* colors, after transformation to *JFN* colors through the equations given in Majewski (1992), for comparison purposes The transformed colors are $(J-F) = 0.75$–0.78, $(F-N) = 0.87$–0.90 for GA, and $(J-F) = 1.06$–1.16, $(F-N) = 0.95$–1.04 for GB, which are within the $(J-F)$ vs. $(F-N)$ distribution in Fig. 17c of Bershady et al. (1994). It is not clear if this difference between the mean colors of galaxies at $z \simeq 0.12$ and those nearby is real or arises from the lack of a precise correction for Galactic absorption and redshift.

5. Summary

With low resolution spectra and CCD images we determined radial velocities and photometric parameters of two small galaxies (GA and GB) in the field of NGC 7479. The radial velocities were calculated using the cross-correlation technique and three sets of templates, in a total of 15 measurements for each galaxy; the mean values were $(35\,513 \pm 413)$ km s^{-1} for NGC 7479-GA and $(38\,009 \pm 83)$ km s^{-1} for NGC 7479-GB

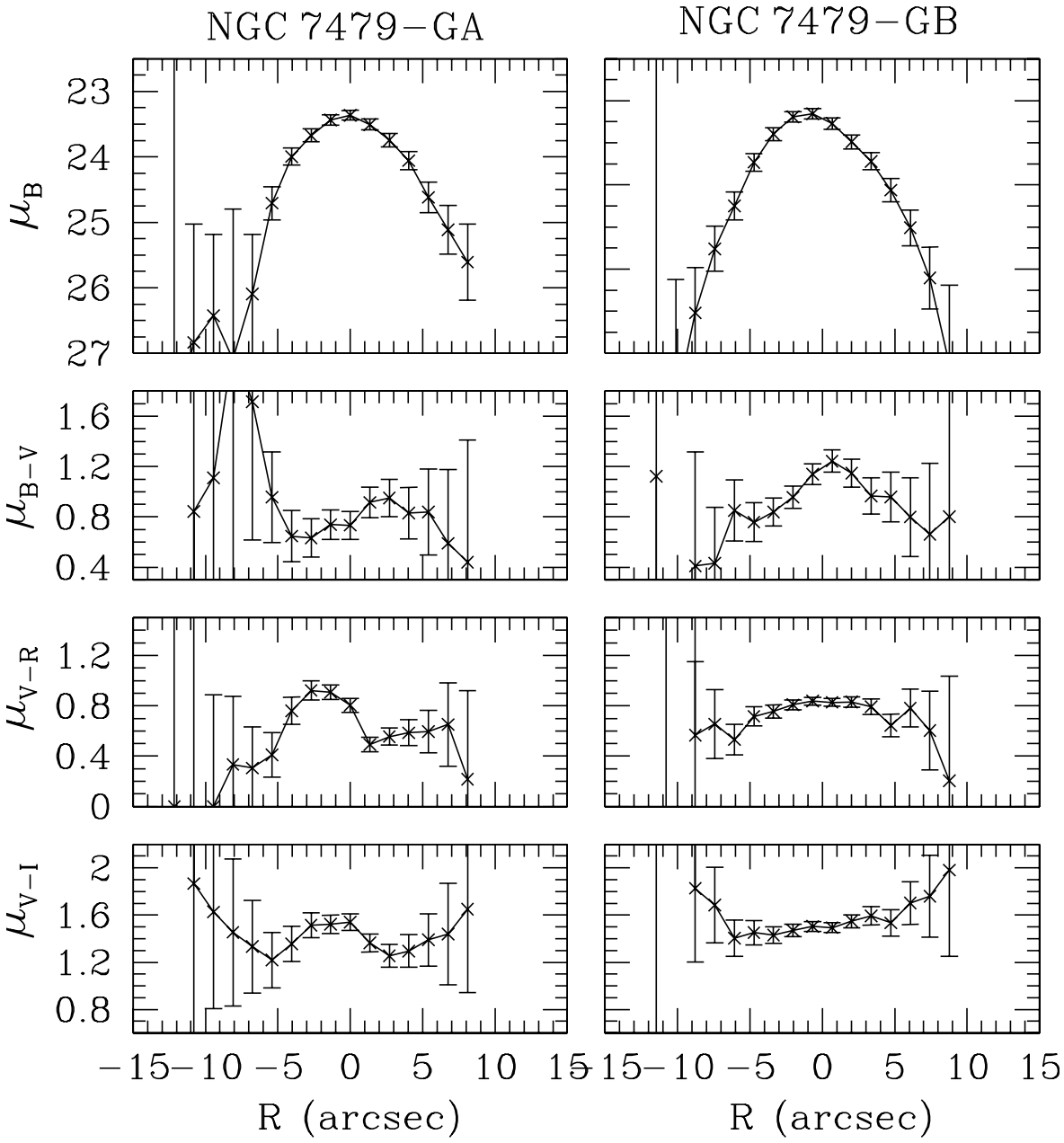

Fig. 6. Surface brightness profiles along the major axis of the galaxies A and B. The position angles are 115° for GA and 87° for GB. The error bars take into account the uncertainty in the sky subtraction.

Table 6. Integrated magnitudes and colors.

Parameter	N7479-GA		N7479-GB	
aperture	10.8″	13.5″	10.8″	13.5″
B	19.27 ± 0.06	19.12 ± 0.06	19.20 ± 0.06	19.03 ± 0.06
V	18.63 ± 0.05	18.49 ± 0.05	18.22 ± 0.04	18.10 ± 0.06
R	17.93 ± 0.04	17.82 ± 0.04	17.44 ± 0.03	17.32 ± 0.03
I	17.16 ± 0.02	17.01 ± 0.03	16.67 ± 0.02	16.52 ± 0.02
$(B-V)$	0.64 ± 0.08	0.63 ± 0.08	0.98 ± 0.07	0.93 ± 0.08
$(V-R)$	0.70 ± 0.06	0.67 ± 0.06	0.77 ± 0.05	0.78 ± 0.07
$(V-I)$	1.47 ± 0.05	1.48 ± 0.06	1.55 ± 0.04	1.58 ± 0.06
B^0	18.33	18.18	18.24	18.07
$(B-V)^0$	0.19	0.18	0.53	0.48
$(V-R)^0$	0.54	0.51	0.63	0.64
$(V-I)^0$	1.16	1.17	1.28	1.31

Despite the large uncertainty, these values indicate clearly that the two faint galaxies are much farther away than NGC 7479, which heliocentric radial velocity is 2381 km s^{-1} (NED – NASA/IPAC Extractragalactic Database).

The photometric analysis yielded isophote parameters, luminosity and color profiles, and integrated magnitudes and colors. Our results suggest that the galaxies have similar sizes and brightnesses, but different morphological types, since GB is significantly smoother and redder than GA.

Assuming a Hubble constant of $H_0 = 75$ km s^{-1} Mpc^{-1}, the derived distances of the galaxies GA and GB are 480 Mpc and 500 Mpc respectively, corresponding to a mean scale $1'' = 2.35$ kpc and mean distance modulus $(m - M) = 38.44$. Using the integrated magnitudes determined in Sect. 4, corrected for redshift, both galaxies have absolute magnitudes around $M_B^o = -19.7$, and major diameters around 30 kpc, which are typical of normal nearby galaxies. Their colors are common among galaxies with similar redshift, but seem to be rare among nearby ones.

Acknowledgements. We deeply thank Dr. Claudia Mendes de Oliveira for clarifying discussion on the subject, as well as for kindly giving us four spectra prior to publication. We thank Dr. Charles Bonatto for careful reading of the manuscript, and the referee, Dr. J. A. Aguerri, for suggestions that really help to improve paper. This research has made use of NASA's Astrophysics Data System Abstract Service (ADS), and the NASA/IPAC Extragalactic Database (NED) which is operated by the Jet Propulsion Laboratory, California Institute of Technology, under contract with the National Aeronautics and Space Administration.

References

Aguerri, J. A. L., Varela, A. M., Prieto, M., & Munoz-Tunon, C. 2000, AJ, 119, 1638
Benedict, G. F. 1982, AJ, 87, 76
Beckman, J. E., & Cepa, J. 1990, A&A, 229, 37
Bershady, M. A., Hereld, M., Kron., R., et al. 1994, AJ, 108, 870
Bica, E. 1988, A&A, 195, 76
Brown, W. R., Geller, M. J., Fabricant, D. G., & Kurtz, M. J. 2001, AJ, 122, 704
Buta, R., & Williams K. L. 1995, AJ, 109, 543
de Vaucouleurs, G., de Vaucouleurs, A., Corwin, H., et al. 1991, The Third Reference Catalogue of Bright Galaxies, (New York: Springer Verlag) (RC3)
Duc, P.-A., & Mirabel, I. F. 1998, A&A, 333, 813
Ho, L., Filippenko, A., & Wallace, L. W. 1997, ApJS, 112, 315
Laine, S., & Gottesman, S. T. 1998, MNRAS, 297, 104
Laine, S., & Heller, C. H. 1999, MNRAS, 308, 557
Keel, W. C. 1983, 269, 466
Laine, S., Kenney, J. D. P., Yun, M. S., et al. 1999, ApJ, 511,709
Landolt, A. U. 1992, AJ, 104, 340
Makarova, L. 1999, A&AS, 139, 491
Majewski, S. R. 1992, ApJS, 78, 87
Martin, P., & Friedli, P., A&A, 326, 449
Martin, P., Lelievre, M., & Roy, J.-R. 2000, ApJ, 538, 141
Poggianti, B. M. 1997, A&A, 122, 399
Puerari, I., & Dottori, H. 1997, ApJ, 476, L73.
Quillen, A. C., Frogel, J. A., Kenney, et al. 1995, ApJ, 441, 549
Rozas, M., Zurita, A., Heller, C. H., et al. 1999, A&AS, 135,145
Saraiva, M. F., Bica, E., & Pastoriza, M. G., et al. 2001, A&A, 376, 43
Schlegel, D. S., Finkbeiner, D. P., & Davis, M. 1998, ApJ, 500, 525
Sempere, M. J., Combes, F., & Casoli, F. 1994, A&A, 299, 371
Tonry, J., & Davis, M. 1979, AJ, 84, 1511
Whitford, A. E. 1971, ApJ, 169, 215